Layer-by-layer self-assembly polyelectrolytes loaded with cyclic adenosine monophosphate enhances the osteo/odontogenic differentiation of stem cells from apical papilla

Jing Zhang[1,2], Irene ShuPing Zhao[3], Ollie YiRu Yu[2], QuanLi Li[1], May Lei Mei[2], ChengFei Zhang[2], Chun Hung Chu[2]

[1]Key Laboratory of Oral Disease Research of Anhui Province, Stomatologic Hospital and College, Anhui Medical University, Hefei, China

[2]Faculty of Dentistry, The University of Hong Kong, Hong Kong, China

[3]School of Stomatology, Shenzhen University Health Science Center, Shenzhen, Guangdong, China

***Key words**: cell encapsulation, layer-by-layer, self-assembly, stem cell, tissue engineering*

Correspondence to : Chun Hung Chu
Faculty of Dentistry
The University of Hong Kong
34 Hospital Road
Hong Kong, China

Email: chchu@hku.hk

ABSTRACT

Objectives: *To utilize layer-by-layer (LBL) self-assembly polyelectrolytes loaded with cyclic adenosine monophosphate (cAMP) and to investigate its effect on the osteo/odontogenic differentiation of stem cells from apical papilla (SCAPs).*

Methods: *SCAPs loaded with cAMP using LBL self-assembly with gelatin and alginate polyelectrolytes (LBL-cAMP-SCAPs). SCAPs, SCAPs treated by LBL without cAMP (LBL-SCAPs) and SCAPs with cAMP in medium (cAMP-SCAPs) were used as control groups. The presence of cAMP and phosphorylation of cAMP-response element-binding protein (CREB) were evaluated by immunofluorescence and western blotting (WB). The release of cAMP and vascular endothelial growth factor (VEGF) were determined by enzyme-linked immuno sorbent assay (ELISA). Cellular morphology was investigated by scanning electron microscopy (SEM). Cell proliferation and viability were assessed by CCK8 and live/dead staining. The odonto/osteogenic differentiation of encapsulated SCAPs was evaluated by Alizarin red staining, quantitative reverse-transcription polymerase chain reaction (RT-PCR) and WB.*

Results: *Immunofluorescence and WB showed LBL-cAMP-SCAPs expressed cAMP and increased the phosphorylation level of CREB. ELISA demonstrated a sustained release of cAMP and VEGF was present up to 14 days. SEM found LBL-coated SCAPs exhibited a spheroid-like morphology. CCK8 and live/dead staining showed that LBL treatment had no significant effect on cell proliferation and viability. LBL-cAMP-SCAPs enhanced mineralized nodule formation and up-regulated the mRNA levels of the osteogenesis-related genes, as well as related transcription factor-2 protein level which were revealed by Alizarin red staining, RT-PCR and WB.*

Conclusions: *LBL self-assembly loaded with cAMP promoted the osteo/odontogenic differentiation of SCAPs.*

Clinical Significance: *LBL self-assembly can be employed as bioactive molecular carrier for tissue regeneration.*

Introduction

Stem cells from apical papilla (SCAPs), which reside in the root apex of developing permanent teeth, contribute to the formation of radicular pulp and root dentin (1). The wide application of SCAPs in bone tissue regeneration is due to they have higher proliferation and multipotent differentiation potentials than dental pulp stem cells (2, 3). Exogenous growth factors and bioactive small molecules addition through systemic administration are reported to induce the multipotent differentiation of SCAPs, such as bone morphogenetic protein (BMP) (4) , insulin-like growth factor 1 (IGF-1) (5), vascular endothelial growth factor (VEGF) (6), cyclic adenosine monophosphate (cAMP) (7) and so on. Genetic modification, like BMP and VEGF gene-co-transfection is an alternative way to augment the osteo/odontogenic differentiation potential of SCAPs (8). Similarly, in our previous study, we confirmed that overexpression of cAMP pathway downstream molecular, cAMP-response element-binding protein (CREB), promoted the osteo/odontogenic differentiation of SCAPs *in vitro* (9). Activation of cAMP pathway has been reported to promote osteogenesis of human mesenchymal stem cells *in vitro* (10). In an ovariectomized mice model, a subcutaneous injection of cAMP substituent once a day increased bone regeneration (11). However, lack of sustainable delivery of cAMP underline the need for mimicking the *in vivo* microenvironment for desired application in clinic.

Layer-by-layer (LBL) self-assembly is a thin-film fabrication coating, which primarily relies on oppositely electrostatic attraction (polycation or polyanion) (12). Cells surface with negative charges attract positively charged polyelectrolyte, and an opposite charge sequentially deposit to form multilayers in the next assembly step. During LBL assembly procedures, charged bioactive molecules can be incorporated into a multiple layer system without loss of bioactivity. Therefore, LBL approach has been applied to controllable drug delivery for encapsulation of fungi (13), bacteria (14) and mammalian cells, like mesenchymal stem cell and neural stem cells (15, 16). We utilized LBL technique to coat collagen and VEGF on titanium surface. The results showed that multilayers by LBL process on a titanium surface promoted the attachment and growth of endothelial progenitor cells *in vitro*, and induced the spontaneous endothelialization of synthetic cardiovascular implants *in vivo* (17).

Gelatin and alginate are electrically charged natural macromolecules, which are effectively utilized in LBL self-assembly reaction. Gelatin derived from denatured collagen is composed of modified natural extracellular matrix components. The amino group of gelatin spontaneously converts into a polycation in water, and is then able to attract carboxyl groups of alginate (18). Alginate is a polysaccharide and possesses excellent cytocompatibility and preferable ability for cell encapsulation (19). Alginate hydrogel enhanced osteogenic potential of dental pulp stem cells, periodontal ligament stem cells and gingival mesenchymal stem cells (20, 21). Therefore, dental-derived stem cells encapsulated by alginate scaffold were considered as a promising approach for bone tissue engineering. Additionally, LBL encapsulation with gelatin and alginate polyelectrolytes was reported has no effect on viability, proliferation or differentiation of neural stem cells (16). However, the application of LBL by gelatin and alginate polyelectrolytes in encapsulation of dental stem cells has rarely been studied.

The aim of this paper is to employ LBL self-assembly technique to encapsulate SCAPs with cAMP.

We hypothesized that SCAPs encapsulated with cAMP using LBL self-assembled gelatin and alginate polyelectrolytes promoted the osteo/odontogenic differentiation of SCAPs *in vitro*, which would contribute significant progress toward the application of bioactive delivery in dental tissue regeneration.

Materials and methods

LBL encapsulation preparation

SCAPs were harvested as described previously (22). SCAPs (2×10^6) were centrifuged in a 15 ml tube to remove the culture medium. 5 ml of 0.1% gelation solution (containing 1 mM cAMP) (Sigma-Aldrich, St Louis, MO, USA) was added to the tube, and the tube was gently centrifuged at 100 r/min for 10 min. Then, the supernatant was discarded after centrifugation at 2000 r/min for 5 min. The cells were washed with 5 ml phosphate-buffered saline (PBS), then the tube was centrifuged again to discard the supernatant. After washing the cells for a second time, 5 ml of 0.1% alginate (Sigma) was added to the tube under centrifugation at 100 r/min for 10 min. Then, the tube was centrifuged for a second time at 2000 r/min for 5 min. The cells were washed with PBS,

and the tube was centrifuged again. After the third layers, 5 ml of 0.1% gelatin (containing 1 mM cAMP) was added. Then, the cells were washed with PBS, and three layers SCAPs were acquired (LBL-cAMP-SCAPs) (Fig. 1). SCAPs encapsulated with gelatin and alginate without cAMP addition were denoted LBL-SCAPs. SCAPs with cAMP added into the medium were denoted as cAMP-SCAPs.

Immunofluorescence staining of cAMP

LBL-cAMP-SCAPs were seeded on the coverslips and fixed in 4 % paraformaldehyde for 10 min at room temperature. After the cells were rinsed with PBS, 0.25 % Triton X-100 was added for permeabilization for 3 min. Then the cells were incubated with 1 % BSA in PBS for blocking for 1 hour. Next, cells were incubated with primary anti-cAMP (EP8471, Abcam, HongKong, China) at 4 ℃ overnight. On the following day, after being rinsed with PBS for three times, secondary antibody (Alexa-488, Abcam) was added for 1 hour in the dark at room temperature. The nuclei were stained with DAPI for 5 min in the dark and rinsed with PBS. Finally, the presence of cAMP on the surface of LBL-cAMP-SCAPs was captured by fluorescent microscope.

Western blot analysis

Cells were lysed in RIPA lysis buffer, containing 1 mM phenylmethylsulfonyl fluoride (PMSF, Beyotime) on ice for 30 min. The denatured proteins (30 μg) from each sample were separated by sodium dodecyl sulfate-polyacrylamide gel electrophoresis (SDS-PAGE) and were then transferred onto 0.22-μm polyvinylidene fluoride (PVDF) membranes (Millipore, Bedford, MA) at 200 mA for 1 hour. After blocking in 5% (w/v) non-fat dried milk dissolved in Tris-buffered saline with Tween (TBST) at room temperature for 1 hour, the membranes were incubated overnight at 4°C with a primary antibody (p-CREB, CREB and Runx 2; Abcam). Finally, the membranes were washed three times for 10 min each with TBST for 10 min before incubation in horseradish peroxidase-conjugated secondary antibodies (1:5000, Santa Cruz, Texas, USA) for 1 hour at room temperature. The protein bands were visualized using enhanced electro chemiluminescence reagent (Advansta, USA). GAPDH (Proteintech, Wuhan, China) was used as an internal control in these experiments.

Enzyme linked immunosorbent assay (ELISA)

To determine cAMP release from the LBL-cAMP-SCAPs, the culture supernatant was evaluated using ELISA (R&D Systems, Minnesota, USA) according to the manufacturer's instructions. The paracrine effect of LbL thin films on VEGF (Dakewe, Shenzhen, China) was also tested using ELISA. At each time interval, supernatants were collected and replaced with an equal volume of fresh medium. Finally, spectrophotometry was used to determine the concentration at 540 nm.

Scanning electron microscopy (SEM) analysis

The cellular morphology of LBL treated SCAPs (LBL-cAMP-SCAPs and LBL-SCAPs), cAMP-SCAPs and SCAPs were analyzed by SEM for time points at 1, 3 and 7 days. Cells were fixed in fixative buffer (containing 2.5% glutaraldehyde) overnight at 4 ℃. After being dehydrated with graded alcohols and dried, the cells were sprayed with gold and viewed using scanning electron microscopy (SEM, Hitachi TM-1000, Japan).

Cell proliferation and viability

The rate of cell proliferation was investigated using Cell Counting Kit-8 (CCK-8; Dojindo, Tokyo, Japan) according to the manufacturer's protocol. Cells at a density of 1×10^4 cells/well were seeded in 96-well plates. At 1, 3, 5, and 7 days, CCK-8 solution was added to the medium for another 4 hours. Absorbance was measured using spectrophotometry at 450 nm to determine the number of viable cells in each well. The background absorbance of wells containing medium and CCK-8 solution but without cells was also measured. The viability was determined after 1, 3 and 5 days of culture using live/dead staining. Acridine orange and propidium iodide solution were dissolved in ethanol to prepare stock solutions with concentrations of 3 μg/ml and 5 μg/ml, respectively. 1 μl of each solution was added into 10 ml of PBS to make a dye mixture. Prior to staining, the medium was discarded, and the cells were washed with PBS three times. Subsequently, 1 ml of working solution was added to each plate for 30 min. Finally, the cells were observed with a fluorescence microscope (TE2000-E, Nikon).

Alizarin red staining

Cells were cultured in a mineralization-inducing medium containing 50 μg/ml ascorbic acid, 10 mM β-glycerophosphate, and 10 nM dexamethasone (Sigma). After 21 days of mineralization induction, the cells were rinsed twice with PBS and fixed with 4% polyoxymethylene for 15 min. Then, the cells were stained with 2% Alizarin red in the dark for 30 min. Photomicrographs of the mineralized nodules were captured. To quantitatively determine the calcium content, 500 μl of 10% cetylpyridinium chloride (Aladdin, Shanghai, China) was added to each well to dissolve the nodules. Aliquots (100 μl) of the supernatant were then measured at an absorbance of 562 nm on a multiplatereader (μQuant MQX200, Bio-Tek).

Quantitative reverse-transcription polymerase chain reaction

The treated cells were cultured in 6-well plates in a mineralization-inducing medium for the times indicated, and total RNA was extracted from the cells in each group using TRIzol reagent (Invitrogen) according to the manufacturer's protocols. For each sample, RNA was subjected to reverse transcription using the PrimeScript II System (Takara, Tokyo, Japan). Quantitative real-time PCR gene expression analyses were performed with the SYBR Premix Ex Taq kit (Takara) using the Mx3000P Real-Time QPCR System (Stratagene, USA). The primers used for the RT-PCR were purchased from Sangon (Shanghai, China) and were as follows:

β-actin (Forward: GCCAAGTGGGTGGTATAGAGG, Reverse: GTGGGATGGTGGGTGTAAGAG), collagen type I (Col I) (Forward: AAGGACAAGAGGCACGTCTG, Reverse: CGCTGTTCTAGTGGTAG), runt-related transcription factor 2 (Runx2) (Forward: CGCCTCACAAACAACCACAG, Reverse:ACTGCTTGCAGCCTTAAATGAC), osteocalcin (OCN) (Forward: GGCAGCGAGGTAGTGAAGAG, Reverse:CTGGAGAGGAGCAGAACTGG), alkaline phosphatase (ALP) (Forward: CCACGTCTTCACATTTGGTG, Reverse: AGACTGCGCCTGGTAGTTGT). The expression level of β-actin was used as an internal control. The relative gene expression values were calculated via the $2^{-\Delta\Delta Ct}$ method.

Statistical analysis

Data were analyzed by statistical SPSS 24.0. One-way analysis of variance was used to compare the difference between experimental groups. The statistical significance was set at *p* value less than 0.05. Data obtained from this study were expressed as the mean ± standard deviation (SD) from at least three independent experiments.

RESULTS

The presence of encapsulated cAMP by LBL

The presence of cAMP on the surface of LBL-cAMP-SCAPs was detected on day 1 to day 7, which were encapsulated with gelatin (containing cAMP) and alginate polyelectrolytes (Fig. 2). Control groups did not show fluorescence of cAMP (data not shown). The results indicated that the successful encapsulation of cAMP. CREB is a down-stream signaling molecule of cAMP pathway. LBL-cAMP-SCAPs group had the greatest amount of phosphorylation of CREB at different time points (Fig. 3A). Compare to cAMP-SCAPs group, phosphorylation of CREB was significantly enhanced in LBL-cAMP-SCAPs group at day 3 (Fig. 3B). The prolonged release of cAMP was assessed by ELISA. LBL-cAMP-SCAPs group exhibited an increasing release profile of cAMP from day 1 to day 14 (Fig. 4A). The results indicated that a sustained cAMP delivery by LBL over a long time period. In addition, the release of VEGF was tested to investigate the paracrine effect of LBL-cAMP-SCAPs. The results showed the release of VEGF increased until 14 days, which was associated with cAMP release (Fig. 4B).

The characterization of encapsulated SCAPs

Cellular morphology was visualized by SEM to observe the LBL coated SCAPs on day 1, 3 and 7 (Fig. 5). At 1 day, LBL-coated SCAPs (LBL-SCAPs and LBL-cAMP-SCAPs groups) expanded slightly and exhibited a spheroid-like morphology, while SCAPs and cAMP-SCAPs stretched broadly and showed a spindle-like morphology. LBL-coated SCAPs exhibited narrow stretching on day 3 and day 7, while control SCAPs fully spread with long filopodia, as shown in Fig. 5. The spreading area in the LBL-treated groups was much more restrained compared with that in the SCAPs group, which was calculated by using Image J (Fig. 6).

To assess whether cellular morphology changes would affect the proliferation of SCAPs, the proliferation of cells was quantitatively evaluated by CCK8 assay. Each group showed similar OD absorbance from day 1 to day 7, revealing that LBL treatment did not influence SCAPs proliferation in a dynamic period (Fig. 7). The viability of the cells in each group was further determined by live/dead staining. Each group showed similar green fluorescence intensity with few dead cells at the indicated times. The result was in accordance with the CCK8 assay, indicating LBL using gelatin and alginate polyelectrolytes had great cytocompatibility (Fig. 8).

The effect of LBL on the differentiation of SCAPs

The calcium content was quantified by alizarin red staining. Fig. 9A showed that more mineralized nodules were deposited in the LBL-cAMP-SCAPs and cAMP-SCAPs groups. The quantitative results of calcium measurements revealed extracellular matrix formation in the cAMP treated groups (Fig. 9B). Consistently, the expression of osteogenic-related genes was further detected by RT-PCR. The mRNA expression level of ALP, Runx2, COL I and OCN were significantly enhanced in the LBL-cAMP-SCAPs and cAMP-SCAPs groups (Fig. 9C-D). Moreover, the LBL-cAMP-SCAPs group expressed highest the protein level of Runx2, as shown in Fig. 10. These above results indicated that encapsulated cAMP using LBL could function as a carrier for cAMP release and was able to successfully induce the osteo/odontogenic differentiation of SCAPs.

Discussion

Stem cells, growth factors and scaffolds are the three crucial components of tissue engineering strategies. To deliver external factors to achieve a long-term effect remains a major challenge. The conventional method used to deliver chemicals is through a systemic administration in the culture medium *in vitro* or administrate an *in vivo* local injection to achieve a rapid release, whereas the drawback is lack of inherent drug delivery (7). To address the need for delivery biomolecule, LBL self-assembly technique were used as a drug carrier to achieve a sustained release of cAMP in this study.

LBL system could incorporate the charged bioactive molecules without compromising their bioactivity (16). It has been widely used for the delivery of growth factors (23), such as IGF-

1 (16), insulin (24), BMP-2 (25) and VEGF (26). It was reported that the release of BMP-2 loaded on a hydroxyapatite scaffold by LBL could last for a period of 4 weeks (25). The release of IGF-1 from LBL polyelectrolyte multilayers coated on titanium implant peaked at 7 days and gradually decreased until 28 days (27). In this study, we first observed the persistency of cAMP on the surface of SCAPs, and the fluorescence intensity gradually decreased from day 1 to day 7. This result verified that the encapsulation of cAMP by LBL was successfully applied on SCAPs. CREB is a downstream molecular of cAMP pathway. Its expression was activated by cAMP loaded by LBL from day 1 to day 7. The result was confirmed by ELISA, which revealed that cAMP release exhibited a burst release within 7 days, followed by a persistent release last for 14 days. The release of encapsulated biomolecules mainly relies on the hydrolysis of LBL films to degrade the entire polyelectrolyte layers (28). As a result, cAMP was released as the gelatin and alginate were hydrolyzed. It was reported that cAMP increased the mRNA expression of VEGF and promoted the vascularization of endothelial cells (29). Enhancement of VEGF release was detected in this study, indicating that cAMP had a paracrine effect on other factor, which may have synergistic effects on regulating cell behaviors. Therefore, these findings provided evidence that LBL films could successfully serve as a reservoir for cAMP delivery.

Morphological analyses revealed that LBL treated SCAPs exhibited a spheroid-like morphology at day 1, and narrowly spread on day 3 and 7. The results indicated the versatile method of cAMP encapsulated by LBL polyelectrolytes above was indeed present. A previous study reported that spheroid formation of adipose-derived stem cells enhanced cell regenerative capacity and delayed cell senescence (30). Therefore, we assessed whether cellular morphology changes would affect stem cell activities. CCK8 assay showed that the pattern of cell growth in LBL-encapsulated SCAPs remained similar to control groups over a dynamic period. Additionally, viability of SCAPs did not notably differ between LBL-encapsulated SCAPs and control groups. It was reported that LBL using gelatin and alginate would not affect the proliferation or viability of MSCs and neural stem cells, due to both of gelatin and alginate display excellent cytocompatibility and have suitable physical properties for bioengineering (16, 26). cAMP pathway is involved in proliferation and apoptosis, which are related to cell type and stimulus concentration. Previous research revealed that activation of cAMP increased the proliferation of stem cell-derived retinal pigment epithelium and neural stem cells (31, 32), while it suppressed

bladder smooth muscle cell proliferation (33). However, in this study, cAMP encapsulated by LBL showed no detrimental effect on SCAPs' proliferation and viability.

cAMP was reported to induce the osteogenic differentiation of MSCs *in vitro* (7, 10). Therefore, LBL self-assembly technique was employed as a cAMP carrier to mimic the *in vivo* microenvironment to achieve a long-term effect. Although cAMP was encapsulated by LBL, it still had an inductive effect on matrix formation, as demonstrated by more calcified nodule formation in the LBL-cAMP-SCAPs group. Runx2 is an osteoblast specific transcription factor that is involved in osteoblast differentiation and bone maturation (34). Notably, cAMP encapsulated by LBL significantly induced the protein expression of Runx2 from 1 week to 3 weeks. In addition, ALP and Col I are two important factors of early osteogenic differentiation, while OCN is regarded as a marker of late stage (35, 36). The analysis of osteogenic genes showed that cAMP encapsulated by LBL enhanced the osteogenic differentiation at the indicated time points. These results confirmed that cAMP loaded by LBL were well-preserved without a loss of intrinsic bioactivity on inducing the osteo/odontogenic differentiation of SCAPs.

cAMP was proven to be an effective factor for inducing the osteo/odontogenic differentiation. However, in order to achieve a local concentration of cAMP *in vivo*, subcutaneous injection of cAMP once a day was performed to increase bone regeneration in ovariectomized mice (7). LBL approach was applied for cAMP delivery to achieve a prolong release in this study. There are two primary ways to apply the LBL technique in regeneration engineering. One is coating the surface of the scaffold or implant to achieve well-compatibility and high differentiation ability (37-39). The surface of the implant loaded with IGF-1 using the LBL technique, which potentially accelerates bone formation in osteoporotic conditions both *in vitro* and *in vivo* (27). Encapsulation of BMP-2 by LBL method on titanium scaffold also enhanced ectopic bone formation (40). Moreover, multilayer films fabricated by LBL on polyethylene terephthalate substrates, significantly promoted human MSCs attachment, proliferation and osteogenic differentiation (41). Alternatively, LBL multilayer films containing chemical stimuli can be used to encapsulate single cell to simultaneously deliver functional molecules. Neural stem cell encapsulated with IGF-1 using LBL promoted the survival and induced the neurogenesis (16). Similarly, it was reported that VEGF-encapsulated mesenchymal stem cells by LBL had a

sustained release of VEGF, thus promoting angiogenesis after transplantation into myocardial infarcted areas of rats (26). Fibroblast growth factor-2 loaded by LBL encapsulated dermal papilla cell exhibited excellent hair follicle regeneration capability *in vivo* (42). In agreement with other reports, we demonstrated that cAMP encapsulated by LBL allowed sustained release of cAMP and had an inductive effect on the osteo/odontogenic differentiation of SCAPs. The results provide a potential strategy for utilizing cAMP encapsulated by LBL in dental regeneration. For the *in vivo* study, animal experiments will be further conducted in the future.

Conclusion

In conclusion, gelatin/alginate loaded with cAMP was prepared to coat SCAPs using LBL self-assembly. The coating showed sustained release of cAMP and had no effect on the proliferation and viability of SCAPs, indicating the biocompatibility of the LBL approach. Moreover, cAMP loaded by LBL resulted in more extracellular matrix formation and osteogenic markers expression, ultimately leading to an enhancing effect on the osteo/odontogenic differentiation of SCAPs. These findings demonstrated that the potential of using LBL as a reservoir for cAMP delivery was able to promote the differentiation of SCAPs, which could be a promising therapy for dental regeneration.

Acknowledgments

This study was supported by the Hong Kong Scholars Program (XJ2016060) and the Health and Medical Research Fund (HMRF) (No:17160402 and No: 06171376) of the Food and Health Bureau of the Hong Kong Government, Hong Kong. The authors have stated explicitly that there are no conflicts of interest in connection with this article.

Figure 1. Schematic of LBL encapsulation process. SCAPs were suspended in gelatin with/without cAMP solution (polycation) for the first layer. After centrifugation, SCAPs were exposed to alginate solution. The polyanion attached to polycation surface to form a second layer. Lastly, SCAPs were added into gelatin with/without cAMP solution again to complete three layers. LBL-SCAPs: SCAPs encapsulated with gelatin and alginate without cAMP. LBL-cAMP-SCAPs: SCAPs encapsulated with gelatin and alginate with cAMP. SCAPs with cAMP added into the medium were denoted as cAMP-SCAPs.

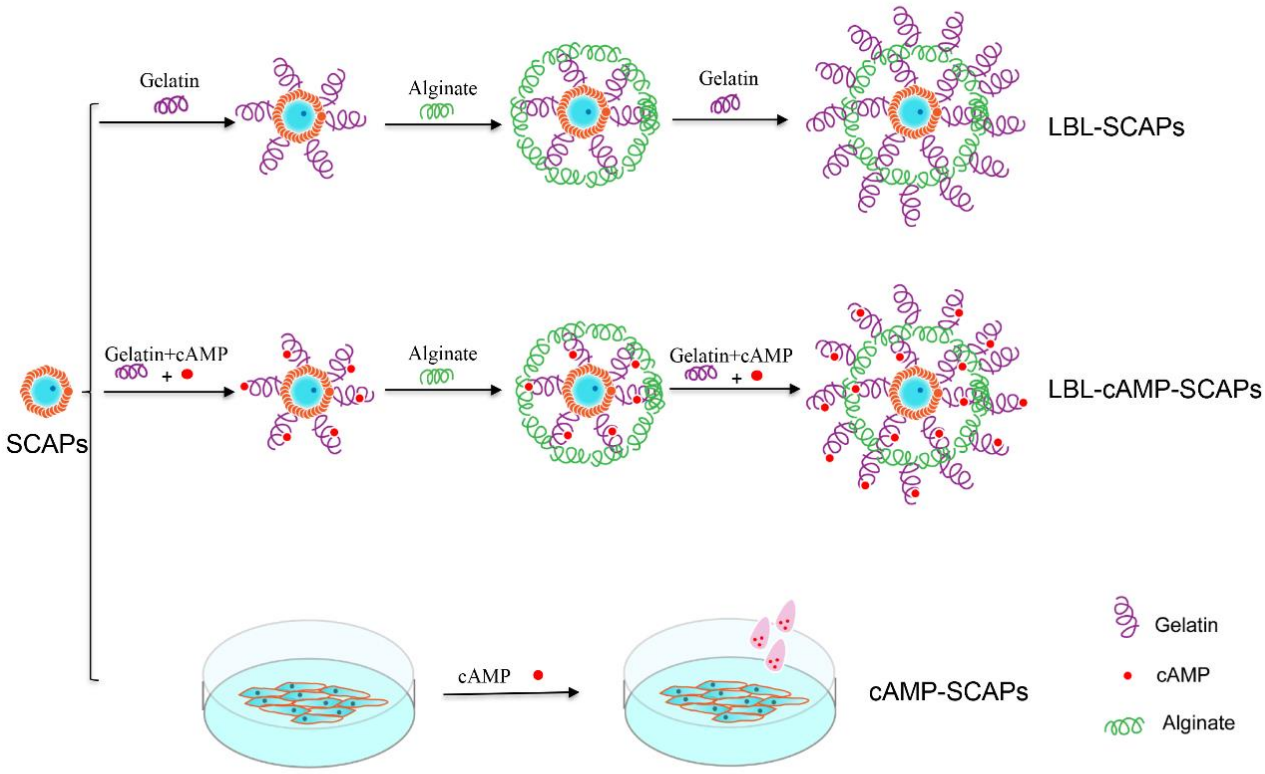

Figure 2. Characterization of LBL-cAMP-SCAPs. Immunofluorescence staining displayed the expression of cAMP on SCAPs. The membrane surface was coated with cAMP (green) while nuclei was stained with DAPI (blue). Scale bar: 200 μm.

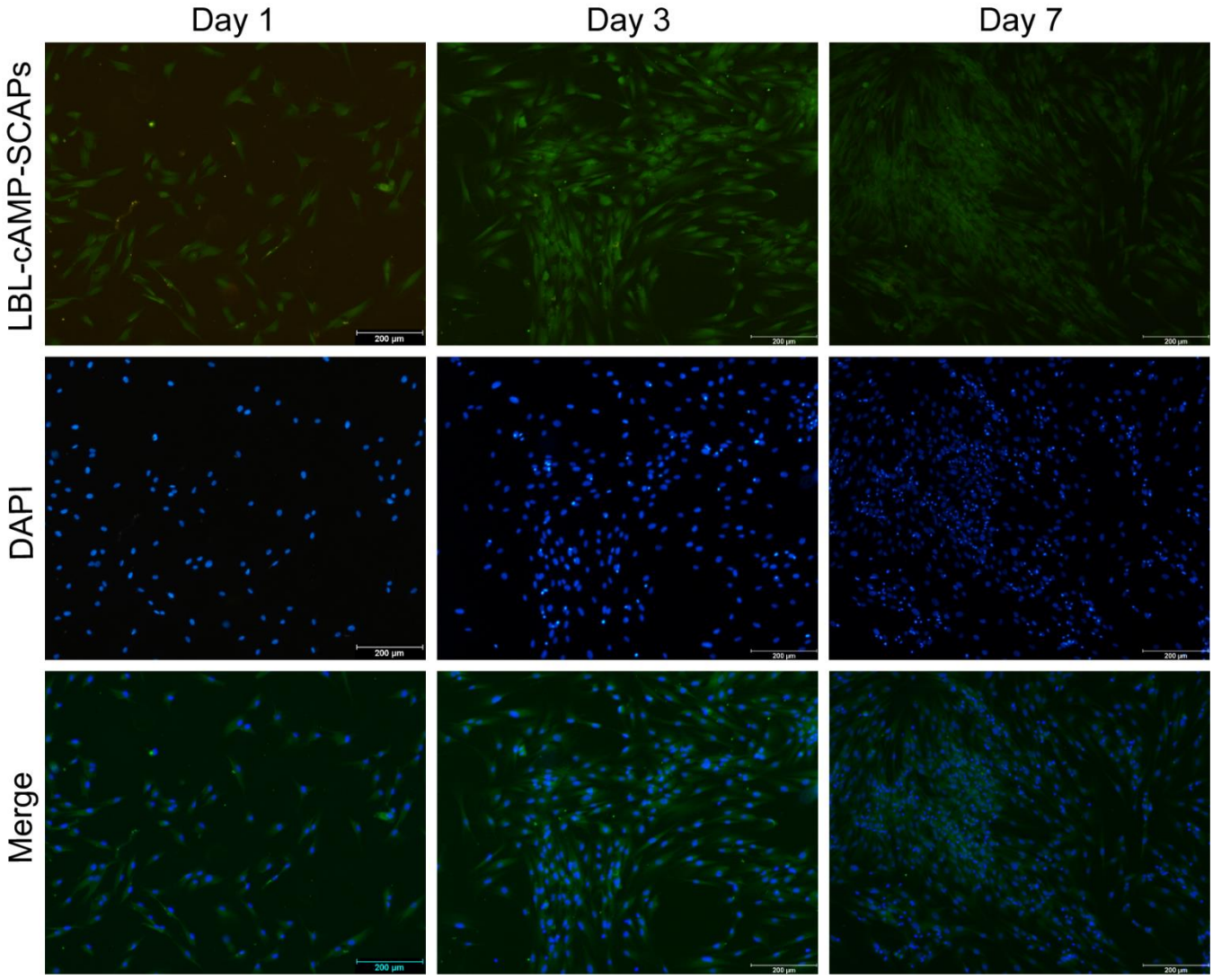

Figure 3. A. Protein expression levels of CREB and p-CREB were determined by western blotting at the indicated time points. GAPDH was used as a loading control. B. Quantification of p-CREB protein levels. $^{**}p<0.01$ and $^{***}p<0.001$ compared with the SCAPs; $^{\#\#}p<0.01$ compared with the LBL-cAMP-SCAPs group. p: phosphorylation.

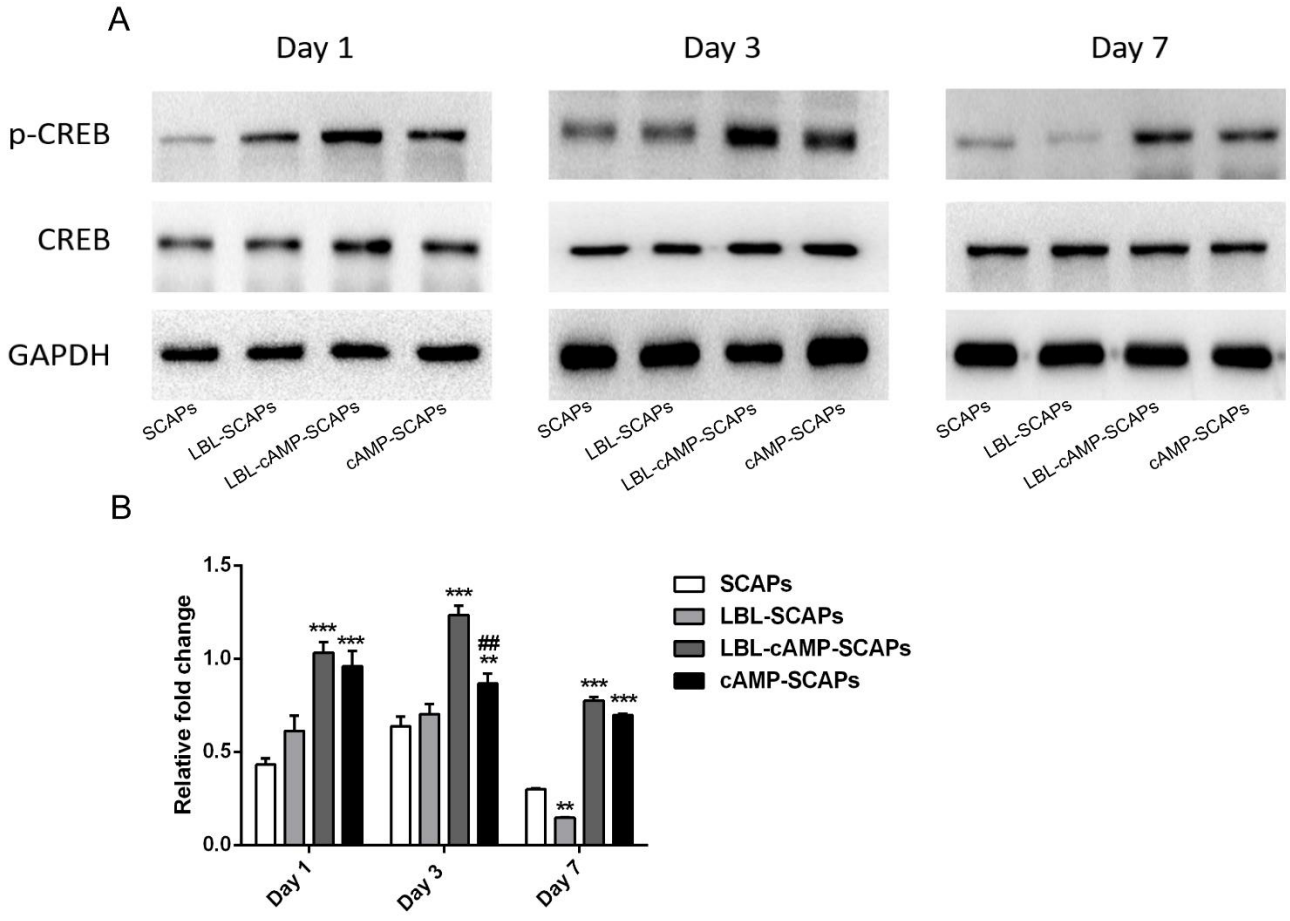

FIGURE 4 (a and b) Cumulative release curves of cAMP and VEGF were detected by ELISA. LBL-cAMP-SCAPs were cultured in 12-well plates. The supernatant was collected at time points from 1 day to 14 days

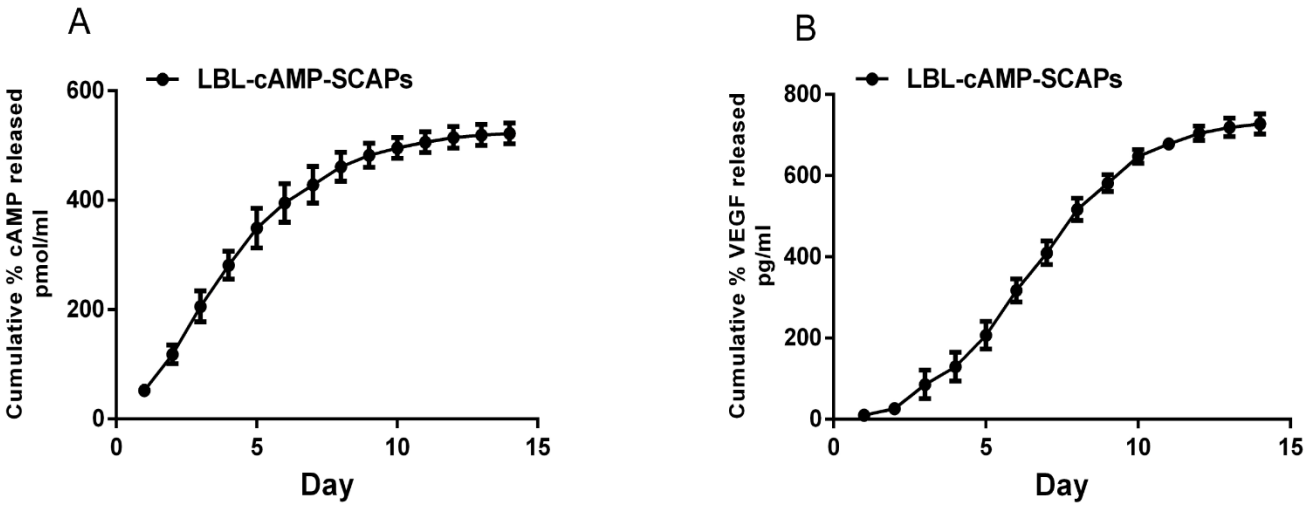

Figure 5. Morphological changes of SCAPs and LBL-loaded SCAPs were detected by SEM on days 1, 3 and 7. SCAPs and cAMP-SCAPs stretched broadly. LBL-SCAPs and LBL-cAMP-SCAPs exhibited a spheroid morphology.

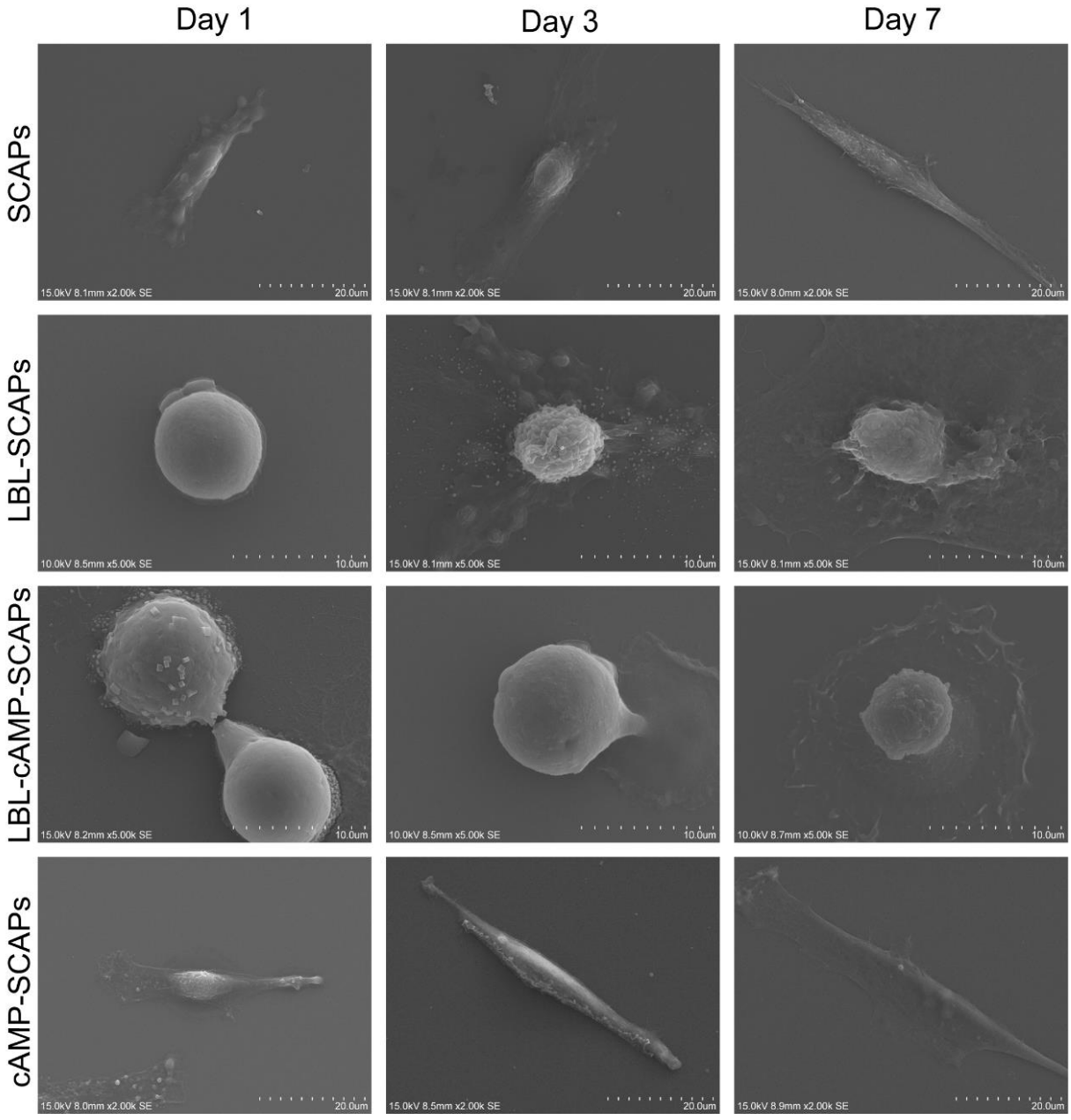

Figure 6. The spreading area of each group was quantified by Image J based on the SEM results. $^{**}p<0.01$ and $^{***}p<0.001$ compared with the SCAPs.

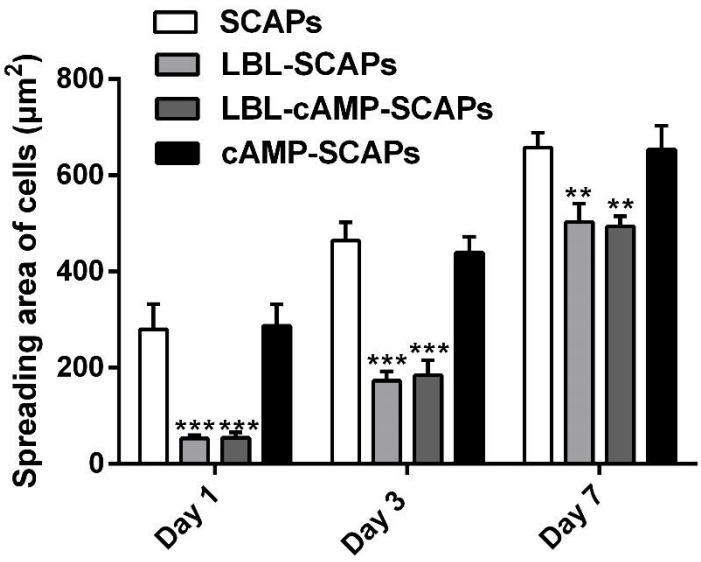

Figure 7. The proliferation of each group at indicated time points was measured by CCK8 assay.

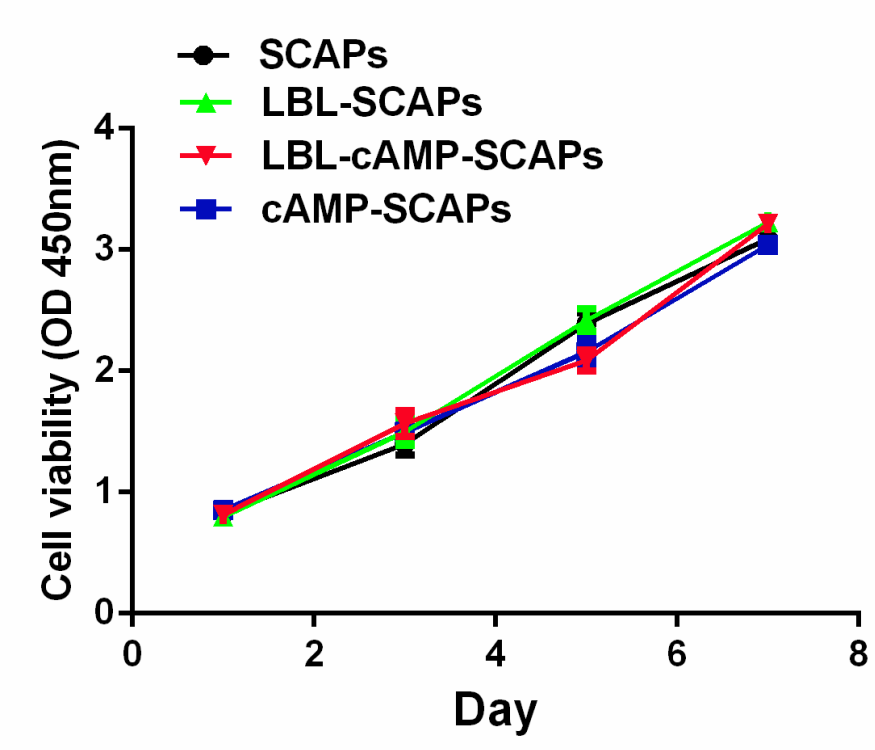

Figure 8. Live/dead staining of SCAPs and LBL loaded SCAPs at the indicated time points was shown on day 1, 3 and 7. Live cells were labeled green.

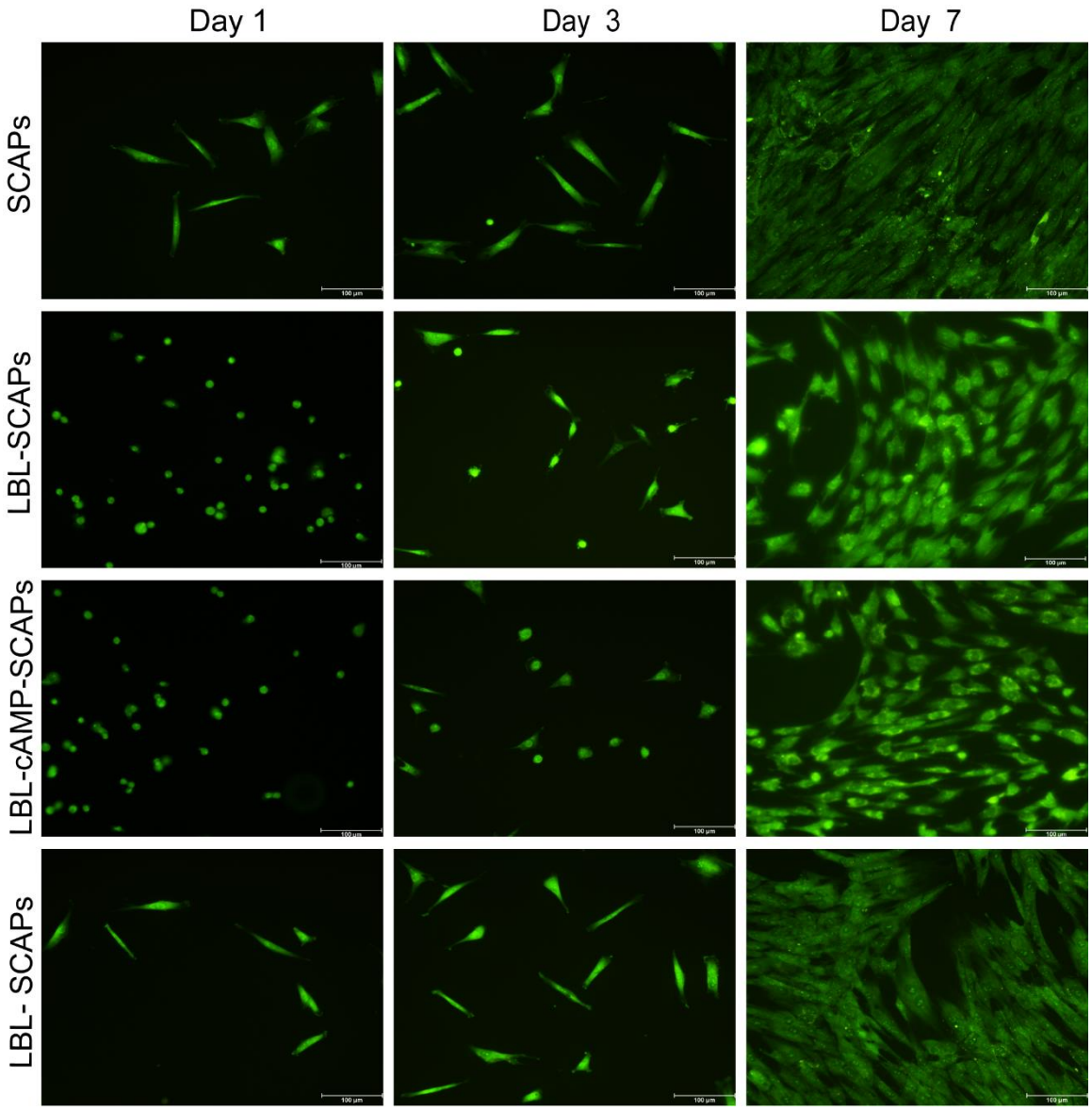

Figure 9. Differentiation of SCAPs and LBL-loaded SCAPs. The cells were cultured in a mineralization-inducing medium for the indicated time. (A) Calcium depositions were assayed via Alizarin red staining. (B) Quantitative analysis of Alizarin red staining. (C-D) Osteogenic gene levels were assayed by RT-PCR. β-actin was used as an internal control. $^{**}p<0.01$ and $^{***}p<0.001$ compared with the SCAPs; $^{\#}p<0.05$ or $^{\#\#\#}p<0.001$ compared with the LBL-cAMP-SCAPs. Scale bars: 500 μm.

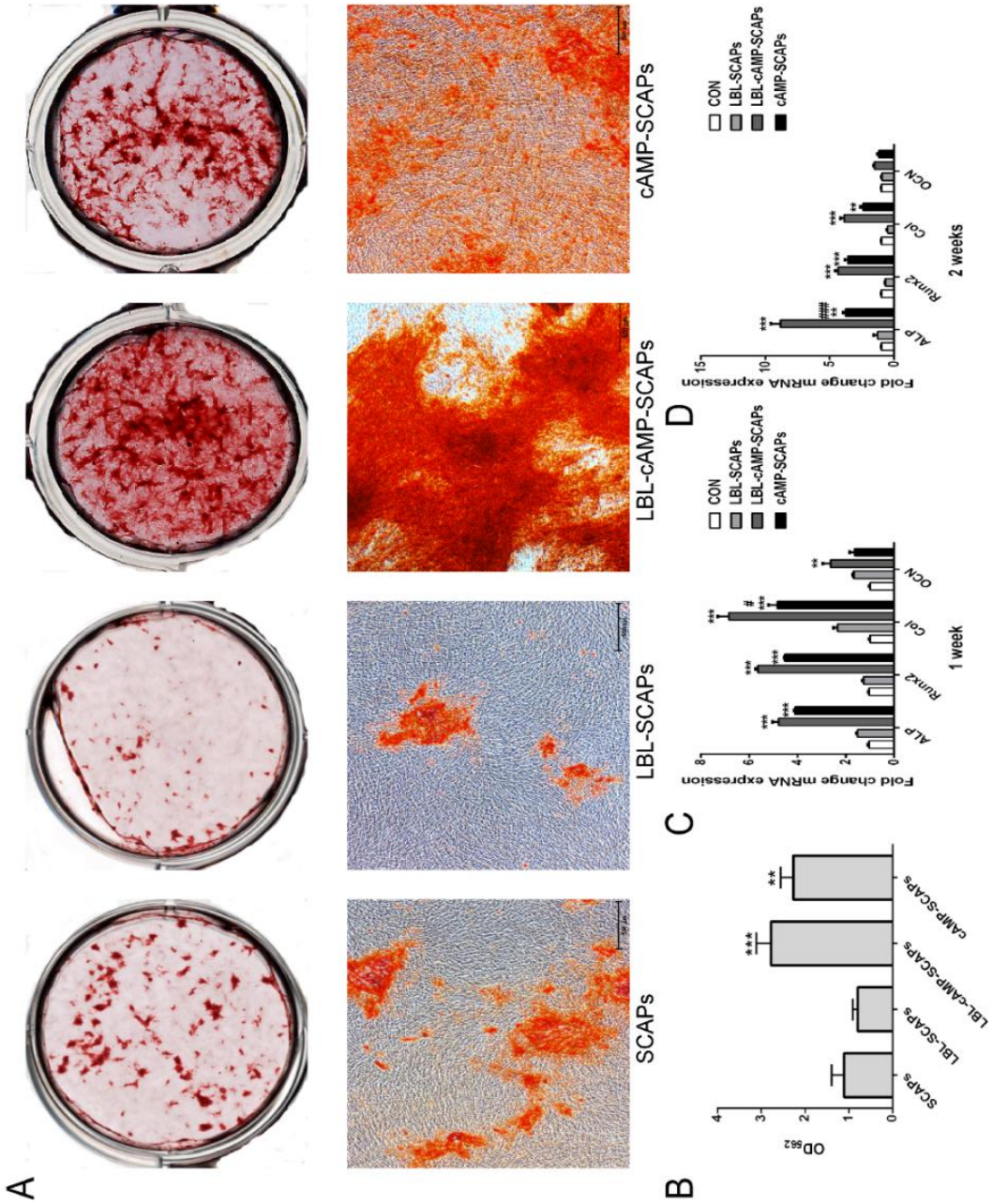

Figure 10. The effect of LBL on the protein expression of Runx2. (A) Protein expression level of Runx2 was determined by western blotting. (B) Quantification of protein levels were shown. $^{**}p<0.01$ and $^{***}p<0.001$ compared with the SCAPs; $^{\#}p<0.05$ compared with the LBL-cAMP-SCAPs.

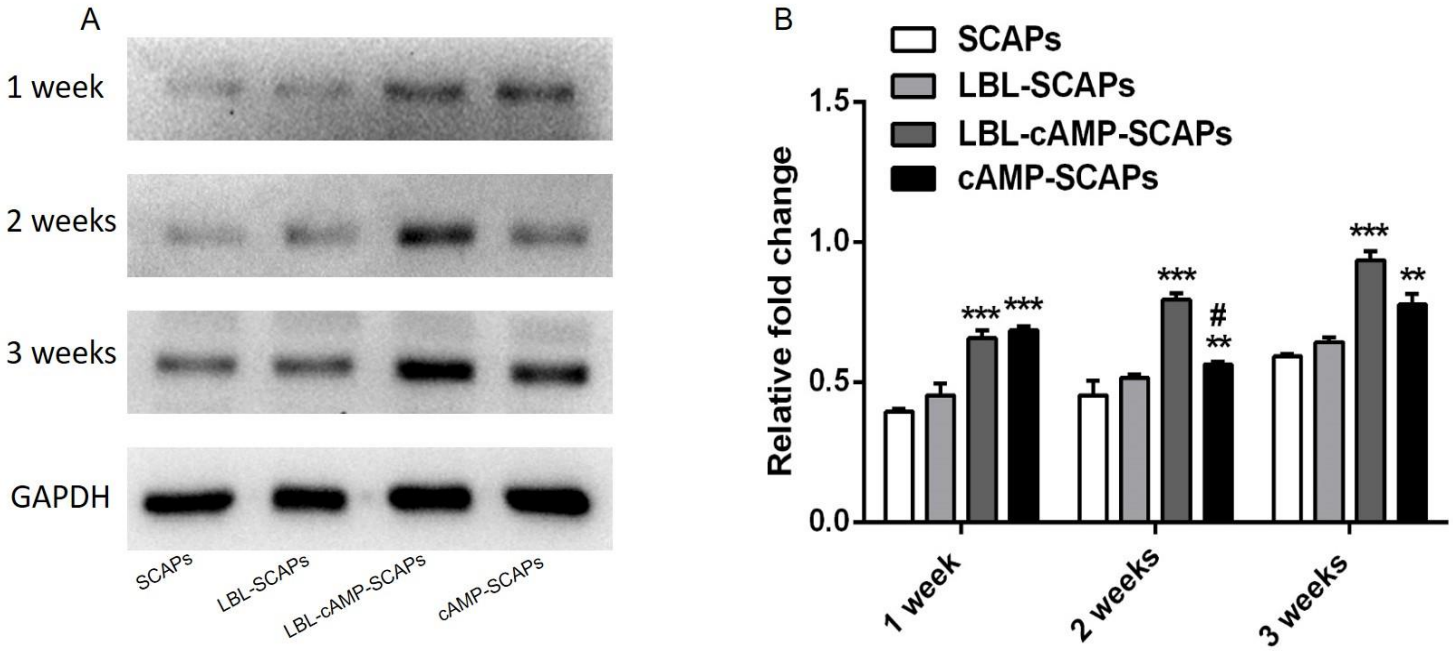

Reference

1. Huang GT, Gronthos S, S. S. Mesenchymal stem cells derived from dental tissues vs. those from other sources: their biology and role in regenerative medicine. J Dent Res 2009;88(9):792-806.
2. Chrepa V, Austah O, A. D. Evaluation of a commercially available hyaluronic acid hydrogel (restylane) as injectable scaffold for dental pulp regeneration: an in vitro evaluation. J Endod. 2017;43(2):257-262.
3. Chopra H, Hans MK, S. S. Stem cells-the hidden treasure: a strategic review. Dent Res J 2013;10(4):421-427.
4. Zhang F, Song J, Zhang H, Huang E, Song D, Tollemar V, et al. Wnt and BMP Signaling Crosstalk in Regulating Dental Stem Cells: Implications in Dental Tissue Engineering. Genes Dis. 2016;3(4):263-276.
5. Wang S, Mu J, Fan Z, Yu Y, Yan M, Lei G, et al. Insulin-like growth factor 1 can promote the osteogenic differentiation and osteogenesis of stem cells from apical papilla. Stem Cell Res. 2012;8(3):346-356.
6. Yadlapati M, Biguetti C, Cavalla F, Nieves F, Bessey C, Bohluli P, et al. Characterization of a vascular endothelial growth factor-loaded bioresorbable delivery system for pulp regeneration. J Endod. 2017;43(1):77-83.
7. Siddappa R, Martens A, Doorn J, Leusink A, Olivo C, Licht R. cAMP/PKA pathway activation in human mesenchymal stem cells in vitro results in robust bone formation in vivo. Proc Natl Acad Sci U S A. 2008;105(20):7281-7286.
8. Zhang W, Zhang X, Ling J, Wei X, Y. J. Osteo-/odontogenic differentiation of BMP2 and VEGF gene-co-transfected human stem cells from apical papilla. Mol Med Rep. 2016;13(5):3747-3754.
9. Su S, Zhu Y, Li S, Liang Y, J. Z. The transcription factor cyclic adenosine 3',5'-monophosphate response element-binding protein enhances the odonto/osteogenic differentiation of stem cells from the apical papilla. Int Endod J. 2017;50(9):885-894.
10. Yang DC, Tsay HJ, Lin SY, Chiou SH, Li MJ, Chang TJ, et al. cAMP/PKA regulates osteogenesis, adipogenesis and ratio of RANKL/OPG mRNA expression in mesenchymal stem cells by suppressing leptin. PLoS One. 2008;3(2):e1540.
11. Kim JM, Choi JS, Kim YH, Jin SH, Lim S, Jang HJ, et al. An activator of the cAMP/PKA/CREB pathway promotes osteogenesis from human mesenchymal stem cells. J Cell Physiol. 2013;228(3):617-626.
12. Tang Z, Wang Y, Podsiadlo P, NA. K. Biomedical Applications of Layer-by-Layer Assembly: From Biomimetics to Tissue Engineering. Adv Mater. 2006;18:3203-3224.
13. Jiang F, Yeh CK, Wen J, Y. S. N-trimethylchitosan/alginate layer-by-layer self assembly coatings act as "fungal repellents" to prevent biofilm formation on healthcare materials. Adv Healthc Mater. 2015;4(3):469-475.

14. Hernandez-Montelongo J, Lucchesi EG, Gonzalez I, Macedo WAA, Nascimento VF, Moraes AM. Hyaluronan/chitosan nanofilms assembled layer-by-layer and their antibacterial effect: A study using staphylococcus aureus and pseudomonas aeruginosa. Colloids Surf B Biointerfaces. 2016;141:499-506.

15. Song G, Hu Y, Liu Y, R. J. Layer-by-Layer heparinization of the cell surface by using heparin-binding peptide functionalized human serum albumin. Materials (Basel). 2018;11(5):pii: E849.

16. Li W, Guan T, Zhang X, Wang Z, Wang M, Zhong W. The effect of layer-by-layer assembly coating on the proliferation and differentiation of neural stem cells. ACS Appl Mater Interfaces. 2015;7(5):3018-3029.

17. Quan LL, Nan Huang, Jia LC, Kai Q, Jun YC, Tian XY, et al. An extracellular matrix–like surface modification on titanium improves implant endothelialization through the reduction of platelet adhesion and the capture of endothelial progenitor cells. J Bioact Compat Polym. 2013;28(1):33-49.

18. Cohen B, Pinkas O, Foox M, M. Z. Gelatin-alginate novel tissue adhesives and their formulation-strength effects. Acta Biomater. 2013;9(11):9004-9011.

19. Augst AD, Kong HJ, DJ. M. Alginate hydrogels as biomaterials. Macromol Biosci. 2006;6(8):623-633.

20. Moshaverinia A, Chen C, Akiyama K, Ansari S, Xu X, Chee WW, et al. Alginate hydrogel as a promising scaffold for dental-derived stem cells: an in vitro study. J Mater Sci Mater Med. 2012;23(12):3041-3051.

21. Kanafi MM, Ramesh A, Gupta PK, RR. B. Dental pulp stem cells immobilized in alginate microspheres for applications in bone tissue engineering. Int Endod J. 2014;47(7):687-697.

22. Sonoyama W, Liu Y, Yamaza T, Tuan RS, Wang S, Shi S, et al. Characterization of the apical papilla and its residing stem cells from human immature permanent teeth: a pilot study. J Endod. 2008;34(2):166-171.

23. Manna U, S. P. Dual drug delivery microcapsules via layer-by-layer self-assembly. Langmuir. 2009;25(18):10515-10522.

24. Yoshida K, Hashide R, Ishii T, Takahashi S, Sato K, J. A. Layer-by-layer films composed of poly(allylamine) and insulin for pH-triggered release of insulin. Colloids Surf B Biointerfaces. 2012;91:274-279.

25. Macdonald ML, Samuel RE, Shah NJ, Padera RF, Beben YM, PT. H. Tissue integration of growth factor-eluting layer-by-layer polyelectrolyte multilayer coated implants. Biomaterials. 2011;32(5):1446-1453.

26. Liu G, Li L, Huo D, Li Y, Wu Y, Zeng L, et al. A VEGF delivery system targeting MI improves angiogenesis and cardiac function based on the tropism of MSCs and layer-by-layer self-assembly. Biomaterials. 2017;127:117-131.

27. Xing H, Wang X, Xiao S, Zhang G, Li M, Wang P, et al. Osseointegration of layer-by-layer polyelectrolyte multilayers loaded with IGF1 and coated on titanium implant under osteoporotic condition. Int J Nanomedicine. 2017;12:7709-7720.

28. Keeney M, Jiang XY, Yamane M, Lee M, Goodman S, F. Y. Nanocoating for biomolecule delivery using layer-by-layer self-assembly. J Mater Chem B. 2015;3(45):8757-8770.

29. Asai J, Takenaka H, Katoh N, S. K. Dibutyryl cAMP influences endothelial progenitor cell recruitment during wound neovascularization. J Invest Dermatol. 2006;126(5):1159-1167.

30. Cheng NC, Chen SY, Li JR, TH. Y. Short-term spheroid formation enhances the regenerative capacity of adipose-derived stem cells by promoting stemness, angiogenesis, and chemotaxis. Stem Cells Transl Med. 2013;2(8):584-594.

31. Choudhary P, Gutteridge A, Impey E, Storer RI, Owen RM, Whiting PJ, et al. Targeting the cAMP and transforming growth factor-β pathway increases proliferation to promote re-epithelialization of human stem cell-derived retinal pigment epithelium. Stem Cells Transl Med. 2016;5(7):925-937.

32. Su C, Wang P, Jiang C, Ballerini P, Caciagli F, Rathbone MP, et al. Guanosine promotes proliferation of neural stem cells through cAMP-CREB pathway. J Biol Regul Homeost Agents. 2013;27(3):673-680.

33. Li K, Yao J, Chi Y, Sawada N, Araki I, Kitamura M, et al. Eviprostat activates cAMP signaling pathway and suppresses bladder smooth muscle cell proliferation. Int J Mol Sci. 2013;14(6):12107-12122.

34. Xu J, Li Z, Hou Y, W. F. Potential mechanisms underlying the Runx2 induced osteogenesis of bone marrow mesenchymal stem cells. Am J Transl Res. 2015;7(12):2527-2535.

35. Leung KS, Fung KP, Sher AH, Li CK, KM. L. Plasma bone-specific alkaline phosphatase as an indicator of osteoblastic activity. J Bone Joint Surg Br. 1993;75(2):288-292.

36. Rickard DJ, Sullivan TA, Shenker BJ, Leboy PS, I. K. Induction of rapid osteoblast differentiation in rat bone marrow stromal cell cultures by dexamethasone and BMP-2. Dev Biol. 1994;161(1):218-228.

37. Oliveira WF, Silva GMM, Cabral Filho PE, Fontes A, Oliveira MDL, Andrade CAS, et al. Titanium dioxide nanotubes functionalized with Cratylia mollis seed lectin, Cramoll, enhanced osteoblast-like cells adhesion and proliferation. Mater Sci Eng C Mater Biol Appl. 2018;90:664-672.

38. Romanelli SM, Fath KR, Phekoo AP, Knoll GA, IA. B. Layer-by-layer assembly of peptide based bioorganic-inorganic hybrid scaffolds and their interactions with osteoblastic MC3T3-E1 cells. Mater Sci Eng C Mater Biol Appl. 2015;51(316-328.).

39. Chen J, Chen C, Chen Z, Chen J, Li Q, N. H. Collagen/heparin coating on titanium surface improves the biocompatibility of titanium applied as a blood-contacting biomaterial. J Biomed Mater Res A. 2010;95(2):341-349.

40. Han L, Wang M, Sun H, Li P, Wang K, Ren F, et al. Porous titanium scaffolds with self-assembled micro/nano hierarchical structure for dual functions of bone regeneration and anti-infection. J Biomed Mater Res A. 2017;105(12):3482-3492.

41. Li Y, Zheng Z, Cao Z, Zhuang L, Xu Y, Liu X, et al. Enhancing proliferation and osteogenic differentiation of HMSCs on casein/chitosan multilayer films. Colloids Surf B Biointerfaces. 2016;141:397-407.

42. Bo-jie Lin, Jin Wang, Yong Miao, Yu-qing Liu, Wei Jiang, Fan， Z-x, et al. Cytokine loaded layer-by-layer ultrathin matrices to deliver single dermal papilla cells for spot-by-spot hair follicle regeneration. J Mater Chem B. 2016;4(3):489-504.